THE IMPACT OF FUEL PARTICLE SIZE DISTRIBUTION ON NEUTRON TRANSPORT IN STOCHASTIC MEDIA

Chao Liang, Andrew T. Pavlou and Wei Ji*
Department of Mechanical, Aerospace, and Nuclear Engineering
Rensselaer Polytechnic Institute
110 8th Street, Troy, NY 12180

ABSTRACT

This paper presents a study of the particle size distribution impact on neutron transport in three-dimensional stochastic media. An eigenvalue problem is simulated in a cylindrical container consisting of fissile fuel particles with five different size distributions: constant, uniform, power, exponential and Gaussian. We construct 15 cases by altering the fissile particle volume packing fraction and its optical thickness, but keeping the mean chord length of the spherical fuel particle the same at different size distributions. The tallied effective multiplication factor (k_{eff}) and flux distribution along axial and radial directions are compared between different size distributions. At low packing fraction and low optical thickness, the size distribution has a significant impact on radiation transport in stochastic media, which can cause as high as ~270pcm difference in k_{eff} value and ~2.6% relative error difference in peak flux. As the packing fraction and optical thickness increase, the impact gradually dissipates.

Key Words: size distribution, eigenvalue problem, particle radiation transport, stochastic media

1. INTRODUCTION

3-D particle systems, characterized by the stochastic distribution of spherical inclusions in a background material, are typical radiation transport media encountered in many scientific and engineering fields. For example, in the area of atmospheric science, solar radiative transfer through clouds consisting of tiny water droplets and dust aerosols is studied. These particles have sizes ranging from 10^{-5} m to 10^{-3} m and their distribution in the cloud can influence the solar energy radiative transfer to the surface of the earth [1]. In the area of nuclear engineering, advanced reactor designs, such as the Very High Temperature Gas-Cooled Reactor [2] and the Fort Saint Vrain Reactor [3], utilize unique fuel elements called TRISO fuel particles that are fabricated to different fuel types (fissile or fertile) and different sizes. These particles are randomly packed in the reactor core at volume packing fractions ranging from 5% to 60%. To provide reliable predictions of solar energy transfer through atmosphere or neutronic safety analysis in nuclear reactors, one needs to model not only the stochastic distribution of particles but the size distribution of each type of particle in the system, which presents a significant computational challenge. Although radiation transport computation in stochastic media, specifically in 3-D particle systems, has been actively researched for a long time [2, 4-6], much of the focus is on the methodology development that accounts for the spatial and size distribution of particles in the media. Less attention was given to the study of particle spatial or size

* Corresponding author, jiw2@rpi.edu Tel: +1 (518) 276 6602; Fax: +1 (518) 276 6025

distribution effects on radiation transport, especially the size distribution effects. Recently, Brantley and Martos [7] have studied a general radiation transport problem to calculate reflection, transmission and absorption rates when radiation penetrates a cubic 3-D particle system, consisting of optically thick spherical particles and an optically thin background at the particle volume packing fractions ranging from 5% to 30%. Spherical particles were assumed to follow three different distributions in radius: constant, uniform and exponential. They found a weak dependence of the predicted radiation transport rates on particle size distribution, provided different distribution functions give the same mean chord length of spherical particles. Earlier work by Olson [8] studied photon transport in 2-D disk and 3-D spherical particle systems and found that very different disk/sphere sizes produced similar predictions of photon transport as long as the total volume packing fractions were the same. Recent work by the University of Michigan [3, 9] on the Fort Saint Vrain reactor has shown the effects of six different distribution functions on the multiplication factors in a densely packed particle system. The radius size distribution range was fixed and different distributions were applied to generate a fuel compact consisting of fuel particles in a packing range of 58% to 60%. No significant differences in multiplication factor were found.

Previous work studied the impact on the integral quantities that depend on the global distribution of particles, such as total absorption rate or multiplication factor. Quantities that depend on the local properties of particle distributions, such as flux distribution, have not been studied before. The flux distribution is important in reactor analysis, because it can be used to identify a hot spot location in the reactor fuel pins that are filled with TRISO fuel particles. In the present paper, we studied the size distribution effect on a simple cylindrical fission system that consists of randomly distributed fissile fuel particles. Five different size distributions are assumed for the fissile particles and their impacts on the multiplication factor, average total flux, and spatial flux distribution in the system are studied. To ensure that the size distribution is the only parametric studied, optimization of the parameters of each distribution function were performed to produce exactly the same mean chord length in the spherical particles.

Our study is focused specifically on neutron transport computation in 3-D particle systems. However, it has a general application to the radiation transport community. First, it can provide a more insightful understanding of the radiation transport phenomena in stochastic media by quantifying the uncertainties in the radiation transport computation due to the uncertainties in particle size. This is fundamental to radiation transport research. Second, from a more practical perspective, it can provide pragmatic guidelines of simplifying the realistic physical model for routine basis analysis. For example, an equivalent single size particle can be used in modeling systems that consist of poly-dispersed particles. This equivalent size is determined by finding an optimal size that produces similar solutions as poly-dispersed distributions with acceptable errors in practice. Keeping a single size for fuel particles in a reactor system is easier to model and efficient for simulations. These considerations have motivated our present work.

The remainder of the paper is outlined as follows: In Section 2, the geometry and material configurations of 3-D particle fission system are described. Specifically, the size distribution of fuel particles and the determination of distribution functions are thoroughly addressed. In Section 3, numerical solutions of effective multiplication factor, average total flux and flux distributions along axial/radial directions are presented for each studied scenario. Comparisons and

interpretations of the results are given. In Section 4, final conclusions and possible future work are presented.

2. CONFIGURATION OF 3-D PARTICLE FISSION SYSTEMS

2.1. Geometric Configuration

We construct a series of 3-D particle fission systems in a cylindrical container of radius 2cm and height 4cm. Fissile fuel particles are randomly packed in the cylinder container with five different radii distributions: constant, uniform, power, exponential and Gaussian. In each distribution, fuel particle radius is distributed over the same range (except for constant distribution) and the mean chord length in fuel particles, denoted as $<l>$, is fixed at 0.05cm by adjusting distribution function parameters. Monte Carlo neutron transport simulations are performed in the system for each distribution of particle size and at five different fuel particle volume packing fractions, denoted as *frac*, of 5%, 15%, 30%, 45% and 60%. A total of 25 geometric configurations need to be constructed. Once a geometry realization of a 3-D particle system is generated, radiation transport simulations are performed in the system.

In our size distribution impact study, we impose two constraints for different fuel particle size distributions: both the size distribution range (except for constant size) and the mean chord length in fuel particles are fixed. These constraints are necessary and reflect pragmatic needs. For example, fabrication of TRISO fuel particles for Fort Saint Vrain has shown that fuel particle size has a distribution between small and large values. Meanwhile, fixing the mean chord length in fuel particles can exclusively allow us to study the size distribution impact only on the radiation transport since neutrons on average see the same optical thickness in fuel and background materials (measured by the product of mean chord length and total cross section in each material). To meet these two constraints, we start with constant size distribution to determine its fuel particle size and mean chord length (as references for other size distributions). Then the size distribution range is determined for other distribution functions by enforcing the range to cover the reference constant size and producing the same mean chord length. We next give a specific description of each radii distribution.

2.1.1. Determination of particle size distribution functions

It was shown by Olson et al. [10] that the probability density function (PDF) for chords in a sphere is given by

$$d(l) = \begin{cases} \dfrac{l}{2 < r^2 >} \displaystyle\int_{l/2}^{R} f(r)dr, & 0 < l < 2R, \\ 0, & 2R < l < \infty, \end{cases} \tag{1}$$

where $f(r)$ is the radii PDF, l is the chord length and R is the maximum value of sphere radius. The value $<r^2>$ is defined in terms of $f(r)$ as $< r^2 >= \int_0^\infty r^2 f(r)dr$.

a) Constant distribution

For constant size distribution of radii,

$$f(r) = \delta(r - R), \tag{2}$$

and we obtain

$$d(l) = \begin{cases} \dfrac{l}{2R^2} \displaystyle\int_{l/2}^{R} \delta(r-R)dr = \dfrac{l}{2R^2}, & 0 < l < 2R, \\ 0, & 2R < l < \infty. \end{cases} \tag{3}$$

The mean chord length is defined by $< l >= \int_0^\infty l d(l) dl$. Then we have $< l >= \dfrac{1}{2R^2}\int_0^{2R} l^2 dl = \dfrac{4R}{3}$. We set R=0.0375cm for constant size distribution and this corresponds to <*l*> = 0.05cm.

b) Uniform distribution

Radii sampling is performed with a uniform distribution with lower endpoint *a* and upper endpoint *b* such that the mean chord length matches the constant size case. The radii distribution PDF for uniform distribution is written as

$$f(r) = \frac{1}{b-a}, \quad a < r < b. \tag{4}$$

The chord length PDF for uniform size distribution fuel particles can be written based on Eq. (1),

$$d(l) = \begin{cases} d_1(l) = \dfrac{l}{2 < r^2 >}\displaystyle\int_a^b f(r)dr, & 0 < l < 2a, \\ d_2(l) = \dfrac{l}{2 < r^2 >}\displaystyle\int_{l/2}^b f(r)dr, & 2a < l < 2b. \end{cases} \tag{5}$$

The mean chord length is $< l >= \int_0^{2a} l d_1(l) dl + \int_{2a}^{2b} l d_2(l) dl = \dfrac{b^4 - a^4}{b^3 - a^3}$. We fix *a* = 0.02cm and then find *b* = 0.04780290771683cm produces a mean chord length of 0.05cm. The range of radius size [*a*, *b*] is used for all other size distribution functions.

c) Power distribution

We choose a power law to sample radii of the form

$$f(r) = (1-p) f_1(r) + p f_2(r), \tag{6}$$

where $f_1(r) = \dfrac{3(r-a)^2}{(R-a)^3}$, $a < r \le R$, $f_2(r) = \dfrac{3(b-r)^2}{(b-R)^3}$, $R < r < b$, and p is the probability of sample a sphere range in [*R*, *b*]. The value of *p* is dependent on the values of *a* and *b*. Here, we want to have the sphere mean chord length at 0.05cm by fixing R =0.0375cm and the values of *a*

and b the same with uniform distribution. The distribution of chord length can be written based on Eq. (1):

$$d(l)=\begin{cases} d_1(l)=\dfrac{l}{2<r^2>}\left[(1-p)\int_a^R f_1(r)dr+p\int_R^b f_2(r)dr\right], & 0<l<2a, \\ d_2(l)=\dfrac{l}{2<r^2>}\left[(1-p)\int_{l/2}^R f_1(r)dr+p\int_R^b f_2(r)dr\right], & 2a<l<2R, \\ d_3(l)=\dfrac{l}{2<r^2>}p\int_{l/2}^b f_2(r)dr, & 2R<l<2b. \end{cases} \quad (7)$$

The mean chord length is then determined by $<l>=\int_0^{2a} ld_1(l)dl+\int_{2a}^{2R} ld_2(l)dl+\int_{2R}^{2b} ld_3(l)dl$. To keep the mean chord length at 0.05cm, p is determined to be 0.47967. Thus,

$$f(r)=0.52033f_1(r)+0.47967f_2(r). \quad (8)$$

d) Exponential distribution

The radii distribution function is expressed as

$$f(r)=\alpha e^{-\beta r}, \quad (9)$$

where the unknown parameters α and β are directly related to each other because the distribution function must satisfy the normalization condition. Using a similar approach as the other sampling schemes, a mean chord length of 0.05cm is achieved for α=36.009 and β=0.034.

e) Gaussian distribution

The radii distribution function is expressed in the form

$$f(r)=(1/\alpha)e^{-\beta(r-R)^2}. \quad (10)$$

A similar procedure as before is performed to determine the mean chord length and the values of α and β that give a mean chord length of 0.05cm: α = 0.027802351 and β = 0.3111.

2.1.2 Construction of 3-D particle systems

After the PDFs for these five fuel particle size distribution functions are determined by fixing the sphere mean chord length at 0.05cm, we can sample the sphere radii and pack them in the container. Due to the difficulty of determining the cumulative distribution function (CDF) of the PDFs, Monte Carlo sampling is performed to accept or reject spheres from the radii distribution functions. If the sampled [r, y] is under the corresponding point [r, f(r)], then r is accepted as sphere's radius; otherwise, it is rejected. This procedure continues until the total volume of the sampled spheres reaches the prescribed volume packing fraction in the cylinder.

For the fuel particle system with volume packing fractions (*frac*) of 5%, 15% and 30%, a fast algorithm based on Random Sequential Addition (RSA) method [11] is used to pack particles into the cylindrical container one-by-one with no overlapping. For the particle system with *frac*= 45% and 60%, a Quasi-Dynamic Method (QDM) [12] is used to generate a high packing system. This method first generates N spatial points that are uniformly distributed within the container for each known sphere center. Then, a normal contact force model is employed to eliminate sphere overlaps while constraining all the spheres within the container boundary.

2.2. Material Configuration

For the studied fuel particle system, we assume the background material is purely scattering with total cross section Σ_t^b=0.4137cm^{-1}, which represents the graphite matrix material in gas-cooled reactors. Spherical fuel particles are composed of fissile materials. For a complete study, three sets of cross section data are assumed in fuel particles. The total cross section of fissile material and the corresponding optical thickness at each cross section set are summarized in Table I.

Table I. Fissile Material Properties in Fuel Particles

frac	$<l>$ (cm)	Σ_t^f (cm^{-1})	$<l>\cdot\Sigma_t^f$	Σ_s^f (cm^{-1})	Σ_f^f (cm^{-1})	v
5%~60%	0.05	2	0.1	1	0.4	2.8
		20	1.0	10	4	
		200	10.0	100	40	

It should be noted that if $<l>$ is the same at all distributions, the mean chord length in the background material within the cylindrical container, $<l_b>$, is also the same. This can be verified by using the Dirac formula [13]: $< l_b >= 4V_b / S_b$, where $V_b=V\cdot(1\text{-}frac)$, V is the total volume of the container and S_b is the total surface area of the background material, calculated as the sum of two areas: the area of the container surface, $S_{cylinder}$, and the area of surfaces of all the fuel particles in the container, $<n_{sphere}>\cdot<S_{sphere}>$. $<n_{sphere}>$ is the average number of fuel particles and can be calculated by $V\cdot frac/<V_{sphere}>$. $<S_{sphere}>$ and $<V_{sphere}>$ are the average surface area and volume of a fuel particle. The mean chord length in the background material can be written as

$$< l_b >= 4V \cdot (1 - frac) / (S_{cylinder} + \frac{V \cdot frac}{< V_{sphere} >} \cdot < S_{sphere} >) \tag{11}$$

Dividing the numerator and denominator by $4V$ and recognizing that the mean chord length in the cylinder is given by $<L>=4V/S_{cylinder}$ and the mean chord length in spheres is $<l>=4<V_{sphere}>/<S_{sphere}>$, we obtain

$$< l_b >= (1 - frac) / (\frac{1}{< L >} + frac \frac{1}{< l >}). \tag{12}$$

From Eq. (12), it can be seen clearly that the mean chord length in the background material in the container is independent of the fuel particle size distributions as long as the mean chord length in the fuel particles is the same.

3. NUMERICAL RESULTS

In this section, we present numerical results for eigenvalue problems in 3-D particle fission systems described in the previous section. An in-house FORTRAN Monte Carlo code was written to solve one-group eigenvalue problems. Table II summarizes the simulation cases for each fuel particle size distribution: five volume packing fractions combined with three sets of cross sections in fuel particles give a total of fifteen cases studied. For each case, a total of 100 independent realizations are generated for radiation transport simulation and final solutions are averaged over 100 realizations. In the simulation of each realization, a total of 2000 fission cycles with 1000 inactive cycles are performed. In each cycle, a total of one million neutron histories are tracked. The effective multiplication factor, total flux and axial/radial flux distributions in the cylindrical container are estimated using collision estimators. These predictions will be compared between different fuel particle size distributions. Then the impact of the spherical size distribution can be studied from comparisons.

Table II. Cases for Eigenvalue Problem

Case	*frac*	Case	$\langle l \rangle \cdot \Sigma_t^f$
1	5%	**a**	0.1
2	15%	**b**	1.0
3	30%	**c**	10.0
4	45%		
5	60%		

3.1. Effective Multiplication Factor

Table III shows values of effective multiplication factor k_{eff} for 15 cases in each size distribution. The standard deviation is kept within 10pcm for all cases. The numbers in bracket show the difference of k_{eff} from the value of constant distribution for the same case.

Table III. Effective Multiplication Factor k_{eff}* (1σ = 10pcm)

Case	Constant	Uniform	Power	Exponential	Gaussian
1a	0.14301	0.14433 (132)	0.14341 (40)	0.14436 (135)	0.14442 (141)
1b	0.73401	0.73674 (273)	0.73497 (96)	0.73672 (271)	0.73670 (269)
1c	1.08504	1.08639 (135)	1.08549 (45)	1.08616 (112)	1.08642 (138)
2a	0.32478	0.32569 (91)	0.32507 (29)	0.32602 (124)	0.32562 (84)
2b	0.99690	0.99697 (7)	0.99691 (1)	0.99691 (1)	0.99690 (0)
2c	1.11334	1.11337 (3)	1.11335 (1)	1.11336 (2)	1.11336 (2)
3a	0.52118	0.52212 (94)	0.52163 (45)	0.52208 (80)	0.52211 (93)
3b	1.07971	1.07980 (9)	1.07982 (11)	1.07979 (8)	1.07981 (10)
3c	1.11848	1.11856 (8)	1.11856 (8)	1.11856 (8)	1.11856 (8)

4a	0.66882	0.66962 (80)	0.66941 (59)	0.66967 (85)	0.66963 (81)
4b	1.10198	1.10214 (16)	1.10201 (3)	1.10214 (16)	1.10214 (16)
4c	1.11954	1.11954 (0)	1.11955 (1)	1.11955 (1)	1.11954 (0)
5a	0.75923	0.75951 (28)	0.75941 (18)	0.75950 (27)	0.75952 (29)
5b	1.10931	1.10944 (13)	1.10941 (10)	1.10944 (13)	1.10944 (13)
5c	1.11978	1.11979 (1)	1.11981 (3)	1.11979 (1)	1.11979 (1)

*The use of parenthesis represents the difference from the constant case in units of pcm. For example, 0.14433(132) is equivalent to 0.14301 + 0.00132.

From Table III, the value of k_{eff} increases with packing fraction and optical thickness in fuel particles for all the radii distributions. The size distribution impact on k_{eff} can be found by comparing the values with the five distributions. Several interesting phenomena are observed: 1) the values of k_{eff} from uniform, exponential and Gaussian distributions are almost the same for all the cases; 2) the constant distribution always gives the smallest value of k_{eff}. The values for the power distribution are the second smallest; 3) the difference among the distributions becomes smaller as the packing fraction and optical thickness increase. For cases 4c and 5c, the values of k_{eff} have no obvious difference. In summary, there is an obvious difference of k_{eff} (as large as 270pcm) in the cases with low packing fractions and low optical thickness. In these cases, the system is more optically thin and more transparent to neutrons.

We can interpret the differences in k_{eff} from the following perspective. Although the same mean chord length in spheres is applied for different distributions, the average size and number of sampled spheres are different at the same volume packing fraction (as shown in Table IV). This difference can result in different degree of neutron channeling when a neutron travels through the gaps (background material) between fuel particles at different size distributions. More fuel particles of a smaller size means less channeling effect since fuel particles can better shield each other. A direct neutronic effect is that the average self-shielding of a fuel particle at different distribution becomes different, leading to the difference in k_{eff}. However, the channeling effect is significant (in affecting the self-shielding) only when the fuel particle volume packing fraction and/or optical thickness are low. At low fuel particle volume packing and/or low optical thickness, neutrons have a high probability of escaping from fuel particles, streaming into the background gaps (channels), and leaking out of the system. At this physical situation, the channeling effect (and fuel particle self-shielding) is very sensitive to the average size and number of sparsely packed fuel particles, which are different at different size distributions. Uniform, exponential and Gaussian distributions produce more fuel particles with smaller average size than constant and power distributions. These fuel particles can shield each other more significantly than bigger size fuel particles. The higher self-shielding results in a reduction in absorption and thus higher k_{eff}. As the packing fraction and fuel particle optical thickness are increased, neutrons have a lower probability of escaping from fuel particles and streaming in the background. Neutron channeling effects become weaker and variations in the average number of fuel particles between distributions are insignificant. The average self-shielding of a fuel particle is primarily affected by the change in optical thickness. The effect of the total number of fuel particles on the self-shielding is minor and therefore the size distribution effect is smaller.

Table IV. Average Number of Spheres for Radii Distributions*

frac	Constant	Uniform	Power	Exponential	Gaussian
5%	11377	13182	11858	13180	13182
15%	34133	39547	35576	39542	39547
30%	68266	79095	71152	79085	79095
45%	102400	118642	106729	118627	118643
60%	136533	158190	142305	158170	158191

*based on the formula $V \cdot frac / \langle V_{sphere} \rangle$, where $\langle V_{sphere} \rangle = \int_a^b (4/3)\pi r^3 f(r) dr$.

3.2. Total Flux and Flux Distribution in Axial and Radial Directions

Total volume average flux is also tallied in the eigenvalue problem and is shown in Table V.

Table V. Total Volume Average Flux in Cylinder [#/cm^2/sec/source particle]

Case	Constant	Uniform	Power	Exponential	Gaussian
1a	2.75e-1	2.69e-1	2.73e-1	2.69e-1	2.70e-1
1b	2.61e-2	2.56e-2	2.51e-2	2.56e-2	2.56e-2
1c	2.42e-3	2.32e-3	2.39e-3	2.31e-3	2.32e-3
2a	9.95e-2	9.77e-2	9.89e-2	9.77e-2	9.72e-2
2b	1.07e-2	1.01e-2	1.02e-2	1.01e-2	1.00e-2
2c	1.07e-3	1.00e-3	1.01e-3	1.00e-3	1.00e-3
3a	4.72e-2	4.54e-2	4.81e-2	4.60e-2	4.54e-2
3b	4.88e-3	4.85e-3	4.86e-3	4.85e-3	4.85e-3
3c	4.86e-4	4.83e-4	4.84e-4	4.83e-4	4.83e-4
4a	2.85e-2	2.67e-2	2.83e-2	2.68e-2	2.68e-2
4b	2.88e-3	2.83e-3	2.83e-3	2.82e-3	2.83e-3
4c	2.86e-4	2.80e-4	2.80e-4	2.80e-4	2.80e-4
5a	1.95e-2	1.95e-2	1.95e-2	1.95e-2	1.95e-2
5b	1.99e-3	1.98e-3	1.97e-3	1.98e-3	1.98e-3
5c	1.99e-4	1.97e-4	1.97e-4	1.97e-4	1.97e-4

A similar phenomenon can be found as was found for k_{eff}: 1) the values of total flux from uniform, exponential and Gaussian distributions are almost the same for all the cases, 2) the constant distribution always gives the largest total flux. The values for the power distribution are the second largest; 3) the difference among the distributions is significant only for cases with low packing fractions and low optical thickness. It is smaller as the packing fraction and optical thickness increase. Also, unlike for k_{eff}, the total flux decreases as optical thickness increases.

Flux distributions along axial and radial directions of the cylindrical container are tallied for the eigenvalue problem. In the axial and radial directions, the cylinder height and radius are uniformly divided into 100 meshes. The volume-average flux in each mesh is calculated and a standard deviation of <1% of relative error is achieved for all the cases. Flux distributions at 5% and 60% packing fractions are shown in Figures 1-2.

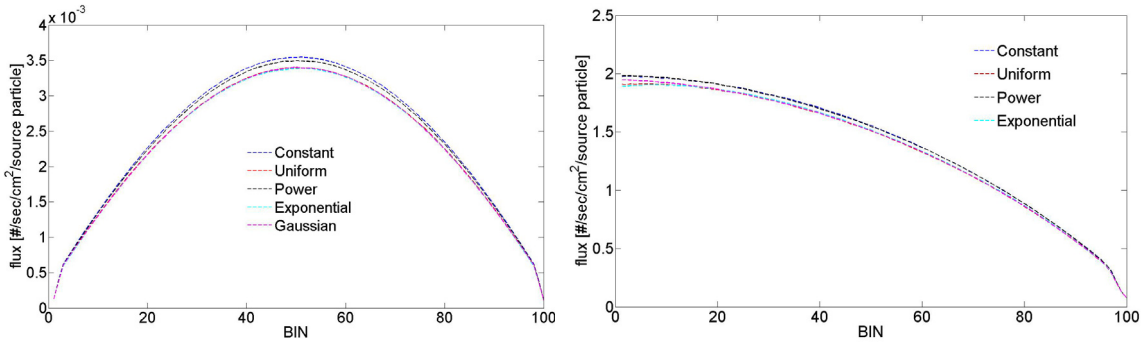

Axial (left) and radial (right) profiles of flux at the optical thickness of 0.1 (Case 1a)

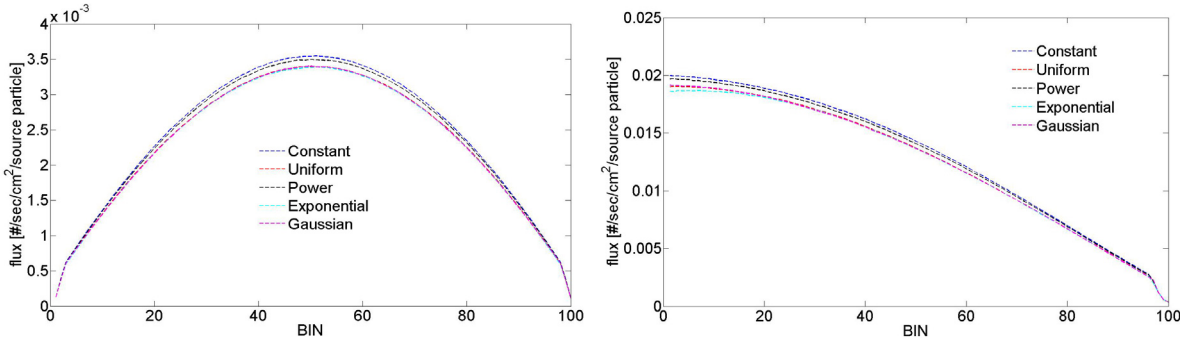

Axial (left) and radial (right) profiles of flux at the optical thickness of 10 (Case 1c)

Figure 1. Axial/Radial flux distributions at 5% packing fraction

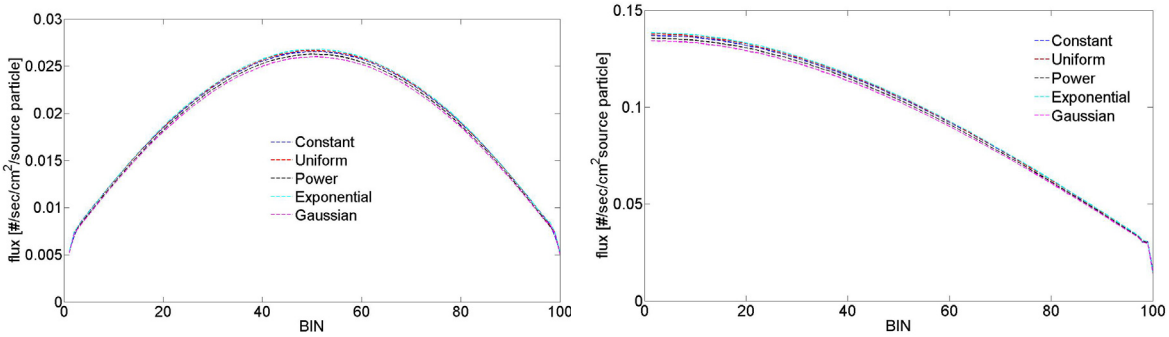

Axial (left) and radial (right) profiles of flux at the optical thickness of 0.1 (Case 5a)

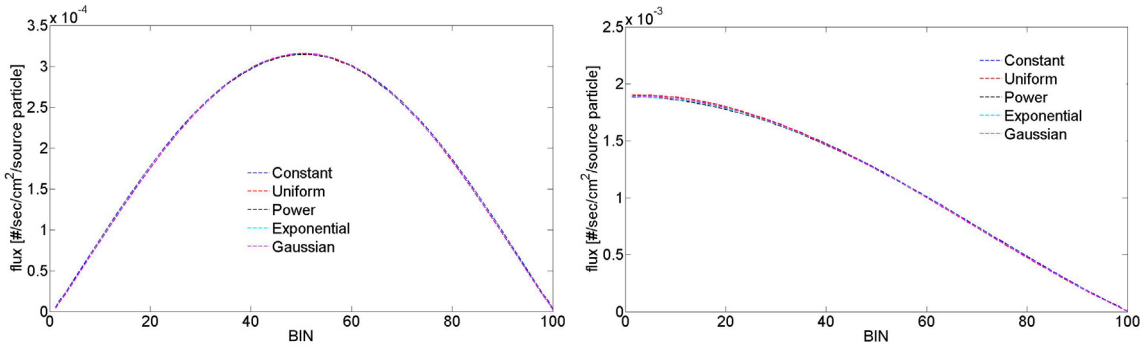

Axial (left) and radial (right) profiles of flux at the optical thickness of 10 (Case 5c)

Figure 2. Axial/Radial flux distributions at 60% packing fraction

From Figures 1-2, we find that, for the low packing fraction and low cross section cases, there is a significant difference among the size distributions. For Case 1a, the peak value of flux with constant distribution is 2.59% larger than the peak value of flux with uniform distribution. However, the difference diminishes as packing fraction and cross section increase. For Case 5c, the difference decreases to 0.35%. This phenomenon is the same as was observed for the multiplication factor. The average number of sampled fuel particles is different from each size distribution at the same packing fraction. At low packing fraction and low optical thickness scenarios, channeling effect between the fuel particles becomes the dominant factor to effect the sensitivity of flux distribution. While as either the increase of the packing fraction or increase of the optical thickness, the channeling effect becomes less important.

4. CONCLUSIONS

In this paper, we investigated the fuel particles' size distribution impact on neutronic behavior in a stochastic medium. A series of radiation transport scenarios in 3-D stochastic particle systems has been constructed. In these stochastic media, particles are composed of fissile material with a specific size distribution. Five radii distributions are adopted for observation in this paper: constant, uniform, power, exponential and Gaussian by keeping the mean chord length in sampled sphere particles the same. Effective multiplication factors and flux distributions are tallied in one group energy MC simulations with variations of two factors: (1) volume packing fraction of the fuel particles in container and (2) optical thickness within the fuel particles. After a thorough comparison of the tallied results, it was found that the channeling effect of the fuel particles dominates the sensitivity of neutron transport in stochastic particle systems.

It was determined that the extent of the channeling effect between the fuel particles is highly dependent on the number of fuel particles. Even with the same volume packing fraction, different size distributions can generate significantly different numbers of fuel particles in the stochastic region. When neutrons transport within a stochastic medium, the case with a higher number of fuel particles has a stronger channeling effect. With the same optical thickness for the five distributions at low packing fraction, neutron channeling out of the stochastic system without interaction with the fuel particles is highly dependent on the fuel particle number. Thus, the tallied results are very sensitive to the size distribution. The variation in size distributions can generate as high as 270pcm difference in k_{eff} value and 2.59% relative difference in peak flux. As the volume packing fraction increases, the probability of neutrons channeling out the system decreases. At very high packing fractions (e.g. 60%), this probability is insignificant.

Similarly, with the same volume packing fraction for the five distributions and at low optical thickness, the size distribution cases with a higher number of fuel particles lead to a much higher interaction probability between neutrons and fuel particles. As optical thickness increases, the interaction probability between neutrons and fuel particles increases. Because of the large number of total particles at high packing fractions, variations in particle number between size distributions become less important to the neutronic behavior.

REFERENCES

1. F.M. Breon, D. Tanre, and S. Generoso, "Aerosol Effect on Cloud Droplet Size Monitored from Satellite," *Science*, **295**, pp.834-838 (2002).
2. W. Ji, J.L. Conlin, W.R. Martin, J.C. Lee, and F.B. Brown, "Explicit Modeling of Particle Fuelfor the Very-high Temperature Gas-cooled Reactor," *Trans. Am. Nucl. Soc.*, **92**, pp.236-238 (2005).
3. A.T. Pavlou, B.R. Betzler, T.P. Burke, J.C. Lee, W.R. Martin, W.N. Pappo, and E.E. Sunny, "Eigenvalue Sensitivity Studies for the Fort St. Vrain High Temperature Gas-Cooled Reactor to Account for Fabrication and Modeling Uncertainties," *Proceeding of PHYSOR 2012,* Knoxville, TN, April 15-20, (2012).
4. I. Murata, A. Takahashi, T. Mori, and M. Nakagawa, "New Sampling Method in Continuous Energy Monte Carlo Calculation for Pebble Bed Reactors," *Journal of Nuclear Science and Technology*, **34**, pp.734-744 (1997).
5. W. Ji and W.R. Martin, "Monte Carlo Simulation of VHTR Particle Fuel with Chord Length Sampling," *Proceeding of Joint International Topical Meeting on Mathematics & Computation and Supercomputing in Nuclear Applications (M&C + SNA 2007)*, Monterey, CA, April 15-19, (2007).
6. C. Liang and W. Ji, "Parameter Sensitivity Study on the Accuracy of Chord Length Sampling Method," *Trans. Am. Nucl. Soc.*, **105**, pp.495-497 (2011).
7. P.S. Brantley and J.N. Martos, "Impact of Spherical Inclusion Mean Chord Length and RadiusDistribution on Three-Dimensional Binary Stochastic Medium Particle Transport," *International Conference on Mathematics & Computational Methods Applied to Nuclear Science and Engineering (M&C 2011)*, Rio de Janeiro, RJ, Brazil, May 8-12, (2011).
8. G.L. Olson, "Gray Radiation Transport in Multi-Dimensional Stochastic Binary Media with Material Temperature Coupling," *Journal of Quantitative Spectroscopy and Radiative Transfer*, **104**, pp.86-98 (2007).
9. T.P. Burke, B.R. Betzler, J.C. Lee, W.R. Martin, A.T. Pavlou, W. Ji and Y. Li, "A Constrained Sampling Methodology for TRISO Microspheres with Continuous Distribution of Diameters," *Trans. Am. Nucl. Soc.,* **107**, pp.516-518 (2012).
10. G.L. Olson, D.S. Miller, E.W. Larsen, and J.E. Morel, "Chord Length Distributions in Binary Stochastic Media in Two and Three Dimensions," *Journal of Quantitative Spectroscopy and Radiative Transfer*, **101**, pp.269-283 (2006).
11. B. Widom, "Random Sequential Addition of Hard Spheres to a Volume," *The Journal of Chemical Physics*, **44**, pp.3888-3894 (1966).
12. Y. Li and W. Ji, "A Collective Dynamics-based Method for Initial Pebble Packing in Pebble Flow Simulations," *Nuclear Engineering and Design*, **250,** pp.229-236 (2012).
13. P.A.M. Dirac, "Approximate Rate of Neutron Multiplication for a Solid of Arbitrary Shape and Uniform Density," Declassified British Report MS-D-5, Part I, (1943).